Electronic structure of FeSi



1995 J. Phys.: Condens. Matter 7 5529

(http://iopscience.iop.org/0953-8984/7/28/010)

J. Phys.: Condens. Matter 7 (1995) 5529–5535. Printed in the UK

# Electronic structure of FeSi

V R Galakhov†, E Z Kurmaev†, V M Cherkashenko†, Yu M Yarmoshenko†, S N Shamin†, A V Postnikov‡‖, St Uhlenbrock‡, M Neumann‡, Z W Lu§, B M Klein§ and Zhu-Pei Shi§

† Institute of Metal Physics, Russian Academy of Sciences, Ural Division, 620219 Yekaterinburg GSP-170, Russia

‡ Universität Osnabrück, Fachbereich Physik, D-49069 Osnabrück, Germany

§ Department of Physics, University of California, Davis, CA 95616-8677, USA

Received 23 March 1995, in final form 10 May 1995

**Abstract.** A full set of high-energy spectroscopy measurements including x-ray photoelectron valence band spectra and soft x-ray emission valence band spectra of both components of FeSi (Fe $K\beta_5$, Fe $L_\alpha$, Si $K\beta_{1,3}$ and Si $L_{2,3}$) are performed and compared with the results of *ab initio* band structure calculations using the linearized muffin-tin orbital method and the linearized augmented plane wave method.

## 1. Introduction

FeSi is a non-magnetic [1] narrow-gap semiconductor [2, 3] at low temperatures. Its magnetic susceptibility $\chi(T)$ increases with temperature and passes through a maximum at $T \sim 500$ K [2]. FeSi becomes metallic above 300 K [3, 4]. The substitution of Co for Fe (about 10% Co) yields a magnet with a helical spin order [5]. Local density functional [6] band structure calculations [7–9] give the correct value of the semiconducting gap (about 0.1 eV), but cannot explain the large magnitude of $\chi(T)$. According to infrared and optical measurements [10], the gap of 50 meV is gradually filled with increasing temperature, with a new spectral weight that cannot be explained within the conventional band structure picture. In connection with a temperature-induced local moment, a model based on unified spin-fluctuation theory was proposed in [11] which explains $\chi(T)$ using a model density of states (DOS).

In spite of the large number of publications devoted to measurements of x-ray photoelectron spectra (XPS) and ultraviolet photoelectron spectra (UPS) of FeSi [12–17], most measurements were performed using polycrystalline samples which do not allow precise measurements on clean surfaces free of contamination. In this paper, we present a full set of precise spectral measurements, including XPS of the valence band and x-ray emission valence spectra for both components of FeSi, which were obtained on the same single crystal, and which provide experimental information about the distribution of total and partial DOS in the valence band.

The already published information on the calculated electronic structure of FeSi presented in [7–9] reveals only total DOS and Fe 3d, Si 3s partial DOS distributions in [8], and Fe 3d, Si 3p DOS for the CsCl-type structure (which is rather different from that known

‖ On leave from Institute of Metal Physics, Russian Academy of Sciences, Yekaterinburg, Russia.

0953-8984/95/285529+07$19.50  

for the bulk FeSi [1]) in [9]. Because of this we performed a new set of band structure calculations of FeSi by two independent methods, linearized muffin-tin orbitals (LMTO) and linearized augmented plane wave (LAPW), which give more detailed information about the total and the Fe 3d, Fe 4p, Si 3s, Si 3d and Si 3p partial DOS distributions.

## 2. Experimental method

The Fe $L_\alpha$ (2p–3d4s transition) x-ray emission spectrum was measured on a RSM-500-type x-ray vacuum spectrometer with a diffraction grating ($N = 600$ lines mm$^{-1}$ and $R = 6$ m) and electron excitation. The spectra were recorded in the second order of reflection by a secondary electron multiplier with a CsI photocathode. The energy resolution was about 0.35–0.40 eV. The x-ray tube was operated at $V = 4.6$ keV, $I = 0.4$ mA.

The Si $K_{\beta_{1,3}}$ (1s–3p transition) x-ray emission spectrum was measured using a fluorescent Johan-type vacuum spectrometer with a position-sensitive detector [18]. The Pd $L$ x-ray radiation from a special sealed x-ray tube was used for the excitation of the fluorescent Si $K_{\beta_{1,3}}$ spectra. A quartz $(10\bar{1}0)$ single crystal curved to $R = 1400$ mm served as a crystal analyser. The spectra were measured with an energy resolution of approximately 0.2–0.3 eV. The x-ray tube was operated at $V = 25$ keV, $I = 50$ mA.

The Si $L_{2,3}$ (2p–3s3d transition) x-ray emission spectra of FeSi were taken from [19], and the Fe $K_{\beta_5}$ (1s–4p transition) x-ray emission spectrum was reproduced from [20].

The XPS valence band spectra of FeSi were measured using a Perkin–Elmer ESCA spectrometer (PHI 5600 ci, monochromatized Al K$\alpha$ radiation). The FeSi single crystal was cleaved in high vacuum prior to the XPS measurements. The XPS spectra were calibrated based on the Au 4f spectra of Au metal ($E_b = 84.0$ eV).

X-ray emission spectra have been brought to the scale of binding energies with respect to the Fermi level using the binding energies of the relevant initial (core-level) states of the x-ray transitions as measured by the XPS technique. Corresponding binding energies are $E_b$(Fe 2p) = 706.7 eV, $E_b$(Si 2p) = 99.3 eV. The values of $E$(Fe $K_{\alpha_1}$) = 6403.86 eV and $E$(Si $K_{\alpha_1}$) = 1740.1 eV were taken for comparison of Fe $L_\alpha$ and Fe $K_{\beta_5}$, Si $L_{2,3}$ and Si $K_{\beta_{1,3}}$ x-ray emission spectra of FeSi.

The measured XPS and x-ray emission spectra are shown in figure 1.

## 3. Calculation details

Electronic structure calculations have been performed for the cubic FeSi structure (eight atoms/cell, space group $P2_13$) as determined in [1] and discussed in detail in [7]. We have used the cubic lattice constant of $a = 4.493$ Å, with Fe atoms occupying the $(0.1358, 0.1358, 0.1358)a$ and equivalent positions of the $B20$ structure, while Si atoms occupy the $(0.844, 0.844, 0.844)a$ and equivalent positions.

In the calculations using the tight-binding LMTO method [21], we used space-filling atomic spheres of equal size on Fe and Si sites ($R = 1.394$ Å) and no empty spheres were introduced. The exchange–correlation potential as proposed by von Barth and Hedin [22] was used. The DOS calculated by the tetrahedron method over 470 $k$-points in the irreducible part of the Brillouin zone are shown in figure 1, and compared with the experimental spectra. Our calculated electron bands are very close to those obtained by Fu and co-workers [8] using the augmented spherical wave method, and our calculated DOS agree well with those of [8, 23]. We found a direct gap of 0.14 eV at the X point of

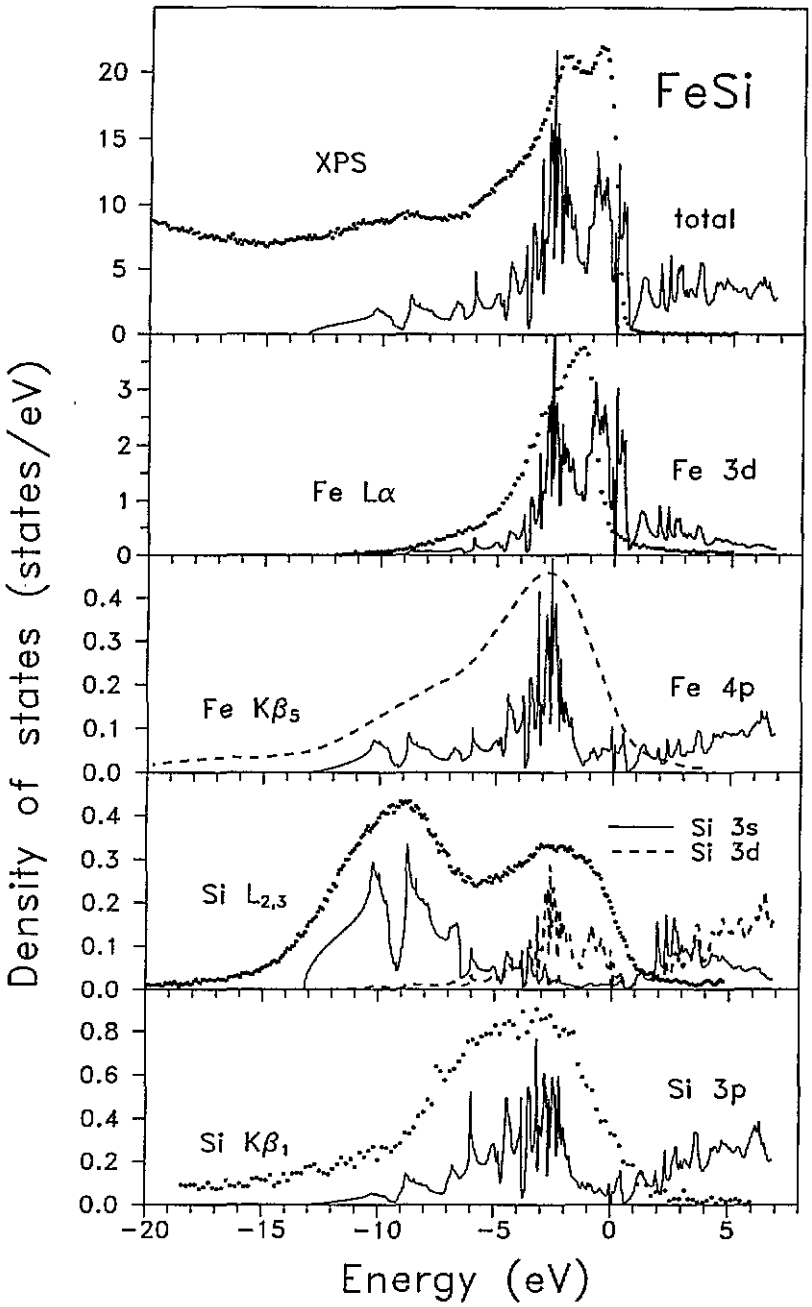


**Figure 1.** Measured XPS spectrum (dots; top panel) and x-ray emission spectra (dots and broken curve for Fe $K_{\beta_5}$; lower panels) of FeSi as compared with total (per unit cell) and partial (per atomic sphere) densities of states calculated using the LMTO method.

the Brillouin zone and an indirect gap of 0.05–0.08 eV, in agreement with the resistivity measurement data reported in [8].

Some small deviations from the bands calculated in [7] using the LAPW method without

any shape approximation imposed on the potential seem to have a quite negligible effect on the densities of states, in the present context of making a comparison with x-ray spectra using the LMTO method. We also carried out an independent LAPW [24, 25] calculation, in which we used the local density approximation [6] form for exchange and correlation given by Ceperley and Alder [26], as parametrized by Perdew and Zunger [27]. In the expansion of the charge density and potential inside the muffin-tin spheres ($R_{Fe} = R_{Si} = 1.111$ Å), lattice harmonics up to angular momentum of $l = 8$ have been used, while the interstitial region was described by a plane wave expansion. Core orbitals were treated self-consistently, retaining, however, only the spherically symmetric part of their density. Scalar relativistic effects (neglecting spin–orbit coupling) were included for the valence states, and full relativistic effects were included for the core states. A large basis set consisting of both real-space orbitals (inside the muffin-tin regions) and plane waves was used. The total number of basis functions used was ~570 per unit cell of eight atoms. The Brillouin zone summations were performed using 24 $k$-vectors in the irreducible section of the Brillouin zone in the self-consistency loop. The densities of states calculated using the LAPW method, with the tetrahedron integration over 176 $k$-points in the irreducible part of the Brillouin zone, are shown in figures 2 and 3. Note that the total DOS calculated in both LMTO and LAPW methods per unit cell (i.e. four formula units) are in good absolute agreement, whereas the partial DOS are somehow smaller in the LAPW calculation (figure 2) because they are attributed to non-overlapping muffin-tin spheres rather than space-filling atomic spheres as in LMTO. The expanded part of the total densities of states plot in the vicinity of the gap is shown at the inset in figure 3. Two sharp peaks formed mostly by Fe d states are separated by the indirect gap of about 0.065 eV.

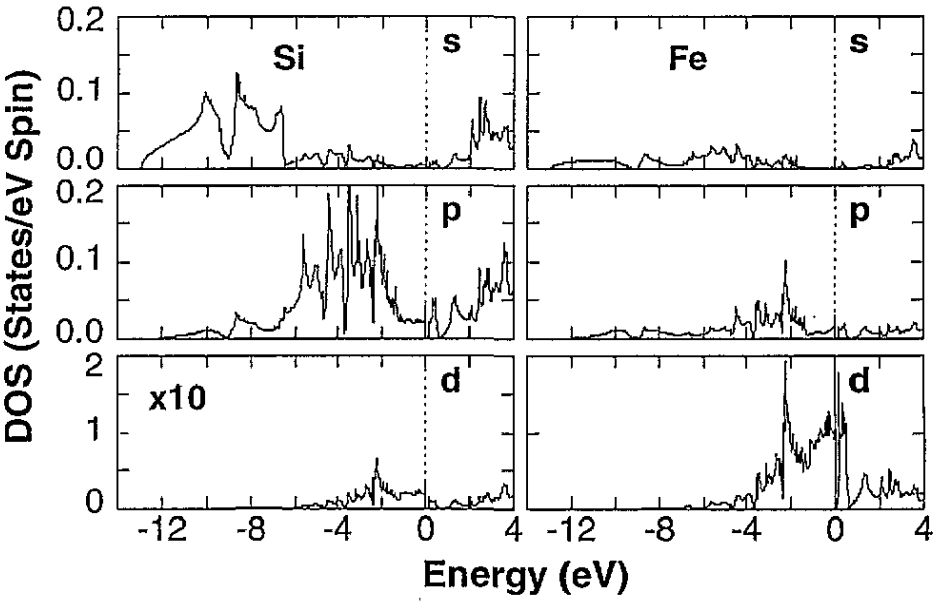


**Figure 2.** Partial densities of states within muffin-tin spheres at Si and Fe sites of FeSi calculated using the LAPW method. Note that the scale for the Fe 3d DOS is different from the rest and that the Si 3d DOS has been multiplied by a factor of ten.

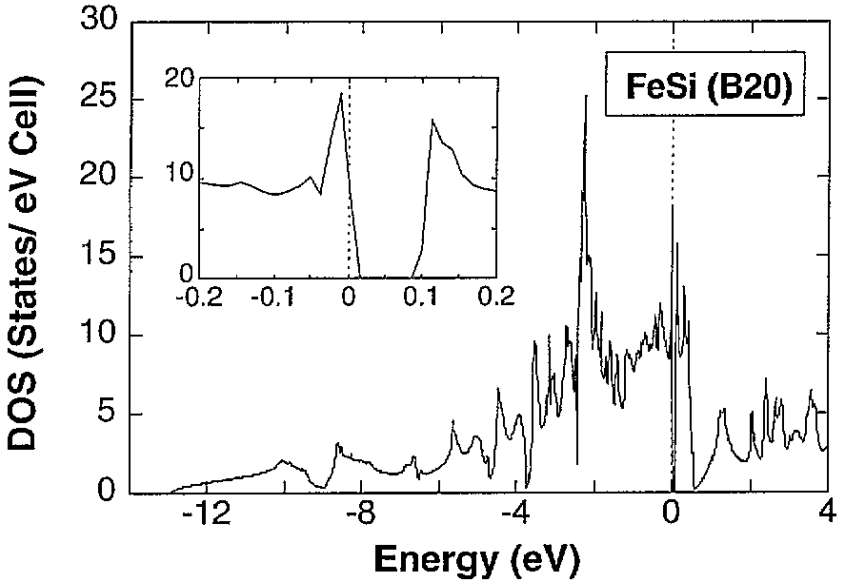


**Figure 3.** Total density of states (DOS) of FeSi calculated using the LAPW method. The inset shows an expanded view of the DOS near the Fermi energy.

There seems to be generally good agreement between the several LDA-based band structure calculation schemes in reproducing the bands, total densities of states and bandwidths in FeSi. Below, we concentrate on discussing particular features of partial densities of states of the constituents as revealed in the x-ray emission spectra and the present calculations.

## 4. Experimental results and discussion

The x-ray photoelectron valence band spectrum and x-ray emission valence band spectra of Fe (Fe $L_\alpha$, Fe $K_{\beta_5}$) and Si (Si $L_{2,3}$, Si $K_{\beta_{1,3}}$) are presented in figure 1. As is known, the XPS valence band spectrum gives information about the total DOS distribution (accurate up to the weight function depending on the atomic photoemission cross-sections, see [28]), whereas the Fe $L_\alpha$, Fe $K_{\beta_5}$, Si $L_{2,3}$, Si $K_{\beta_{1,3}}$ x-ray emission spectra (in accordance with dipole selection rules) give information about partial Fe 3d4s, Fe 4p, Si 3s3d and Si 3p densities of states, respectively. These spectra are compared in figure 1 with the results of the LMTO band structure calculations by aligning the calculated and experimental positions of the Fermi level. We note that the experimental XPS valence band spectrum reproduces the total DOS distribution of FeSi quite well. In particular, it is very important that in our experiments we have found the splitting of the main peak of the XPS spectrum in the range 0–2 eV, which corresponds to the Fe 3d band splitting. This distinct splitting was not found previously in XPS [12] or UPS [13, 14, 16, 17] measurements on FeSi, and its absence was attributed in [17] to a hole lifetime broadening which increases with binding energies. The similar splitting of the XPS valence band spectrum of FeSi was found in [15] only in the measurements done at low temperatures ($T = 120$ K). In our opinion, this discrepancy between fine structure in the present and previous XPS (UPS) valence band spectra is due to the high quality of the FeSi single crystal which was used for the present measurements.

The low-energy Si 3p and Si 3s subbands are reflected in the XPS valence band spectrum as low-intensity (due to low values of respective photoionization cross sections [28]) features located at binding energies of approximately 4.5 and 9 eV, respectively.

The experimental Fe $L_\alpha$ x-ray emission spectrum reproduces fairly well the position of the centre of gravity of the calculated Fe 3d DOS distribution in the valence band of FeSi, but not the splitting of the Fe 3d band. This is due to the large total distortion of the Fe $L_\alpha$ x-ray emission spectrum which includes the instrumental distortion (about 0.4 eV) and the width of the inner (core) Fe 2p level (about 0.8–1.0 eV) which is determined by the lifetime of the core-level vacancy under an x-ray transition.

The experimental Fe $K_{\beta_5}$ spectrum shows two maxima located at binding energies of approximately 3.5 and 9.0 eV, which is in accordance with the theoretical distribution of the Fe 4p partial DOS. It is also seen from both the theoretical and experimental spectra that Fe 4p states are hybridized mostly with Si 3p and Si 3d states.

The experimental Si $L_{2,3}$ x-ray emission spectra corresponds to the 2p–3s3d transition. Usually it is considered that the Si 3d states do not take part in the chemical bonding in 3d transition metal silicides. As was emphasized in [19], the high-energy subband of Si$L_{2,3}$ x-ray emission spectra of transition metal silicides FeSi, MnSi and NiSi, as well as that of disilicides $FeSi_2$, $MnSi_2$ and $NiSi_2$, cannot be explained without the assumption that Si 3d states contribute to the chemical bonding. Subsequently, the same conclusion was drawn for Pt silicides ($Pt_2Si$, PtSi) in [29] based on an analysis of the Si $L_{2,3}$ x-ray emission spectra of these compounds. This conclusion is now again confirmed for FeSi by two independent sets of band structure calculations (see figures 1 and 2). One can see from figure 1 that the Si 3s DOS is concentrated in the range of binding energies about 6–13 eV where the most intensive low-energy subband of the Si $L_{2,3}$ x-ray emission spectrum is located. The centre of gravity of the Si 3d states distribution corresponds to a binding energy about 2 eV where the high-energy maximum of the Si $L_{2,3}$ spectrum is situated. The Si 3d states are strongly hybridized with Fe 3d states, and the same splitting of the Si 3d band (about 2 eV) as that in the Fe 3d subband is observed in the band structure calculations.

The energy position and fine structure of the Si $K_{\beta_{1,3}}$ x-ray emission spectrum is in good accord with the Si 3p partial DOS distribution (see figure 1).

## 5. Conclusion

The results of high-energy spectroscopy measurements of FeSi single crystals, including the XPS valence band spectrum and the x-ray emission valence band spectra of both constituents, were presented. They were compared with two independent *ab initio* band structure calculations of FeSi, performed using the LMTO and LAPW methods, and good agreement between the experimental and theoretical spectra was found.

## Acknowledgments

The authors are grateful to Castor Fu for sending his data on the calculated density of states of FeSi. AVP, StU and MN appreciate the financial support of the Deutsche Forschungsgemeinschaft (SFB 225, Graduate College). This work was supported by the Russian Foundation for Fundamental Research (grant No 94-03-08040) and NATO International Scientific Exchange Program (project HTECH LG 940861). ZWL, BMK and ZPS are grateful for support by the University Research Funds of the University of California at Davis.

## References


[1] Watanabe H, Yamamoto H and Ito K 1963 *J. Phys. Soc. Japan* **18** 995
[2] Jaccarino V, Wertheim G K, Wernick J H, Walker L R and Arajs S 1967 *Phys. Rev.* **160** 476
[3] Kaidanov V I, Tselishchev V A, Iesalniek I K, Dudkin L D, Voronov B K and Trusova N N 1968 *Sov. Phys.–Semicond.* **2** 382
[4] Wolfe R, Wernick J H and Haszko S E 1965 *Phys. Lett.* **19** 449
[5] Beille J, Voiron J and Roth M 1983 *Solid State Commun.* **47** 399
[6] Hohenberg P and Kohn W 1964 *Phys. Rev.* **136** B864
Kohn W and Sham L J 1965 *Phys. Rev.* **140** A1133
[7] Mattheiss L F and Hamann D R 1993 *Phys. Rev.* B **47** 13 114
[8] Fu C, Krijn M P C M and Doniach S 1994 *Phys. Rev.* B **49** 2219
[9] Girlanda R, Piparo E and Balzarotti A 1994 *J. Appl. Phys.* **76** 2837
[10] Schlesinger Z, Fisk Z, Zhang H-T, Maple M B, Di Tusa J F and Aeppli G 1993 *Phys. Rev. Lett.* **71** 1748
[11] Takahashi Y and Moriya T 1979 *J. Phys. Soc. Japan* **46** 1451
[12] Speier W, von Leuken E, Fuggle J C, Sarma D D, Kumar L, Dauth B and Buschow K H J 1989 *Phys. Rev.* B **39** 6008
[13] von Känel H, Mäder K A, Müller E, Onda N and Sirringhaus H 1992 *Phys. Rev.* B **45** 13 807
[14] Chainani A, Yokoya T, Morimoto T, Takahashi T, Yoshii S and Kasaya M 1994 *Phys. Rev.* B **50** 8915
[15] Oh S-J, Allen J W and Lawrence J M 1987 *Phys. Rev.* B **35** 2267
[16] Kaklizaki A, Sugawara H, Nagakura I, Ishikawa Y, Komatsubara T and Ishii T 1982 *J. Phys. Soc. Japan* **51** 2597
[17] Saitoh T, Sekiyama A, Mizokawa T, Fujimori A, Ito K, Nakamura H and Shiga M 1995 *Phys. Rev. Lett.* submitted
[18] Dolgih V E, Cherkashenko V M, Kurmaev E Z, Goganov D A, Ovchinnikov E K and Yarmoshenko Yu M 1984 *Nucl. Instrum. Methods* **224** 117
[19] Kurmaev E Z, Fedorenko V V, Shamin S N, Wiech G and Kim Y 1992 *Phys. Scr.* T **41** 288
[20] Kolobova K M 1970 *PhD Thesis* Institute of Metal Physics, Sverdlovsk
[21] Andersen O K and Jepsen O 1984 *Phys. Rev. Lett.* **53** 2571
Andersen O K, Pawlowska Z and Jepsen O 1986 *Phys. Rev.* B **34** 5253
[22] von Barth U and Hedin L 1972 *J. Phys. C: Solid State Phys.* **5** 1629
[23] Fu C private communication
[24] Andersen O K 1975 *Phys. Rev.* B **12** 3060
Wimmer E, Krakauer H, Weinert M and Freeman A J 1981 *Phys. Rev.* **24** 864
Hamann D R 1979 *Phys. Rev. Lett.* **42** 662
Wei S-H and Krakauer H 1985 *Phys. Rev. Lett.* **55** 1200
Wei S-H, Krakauer H and Weinert M 1985 *Phys. Rev.* B **32** 7792
[25] Singh D J 1994 *Planewaves, Pseudopotentials and the LAPW Method* (Dordrecht: Kluwer)
[26] Ceperley D M and Alder B J 1980 *Phys. Rev. Lett.* **45** 566
[27] Perdew J P and Zunger A 1981 *Phys. Rev.* B **23** 5048
[28] Yeh J J and Lindau I 1985 *At. Data Nucl. Data Tables* **32** 1
[29] Yamauchi S, Hirai M, Kusaka M, Iwami M, Nakamura H, Ohshima H and Hattori T 1994 *Japan. J. Appl. Phys.* **33** L1012